Available online at www.sciencedirect.com
ScienceDirect
Quaternary International 198 (2009) 19–36

High-resolution record of the last climatic cycle in the southern Carpathian Basin (Surduk, Vojvodina, Serbia)

Pierre Antoine[a,*], Denis-Didier Rousseau[b,c], Markus Fuchs[d], Christine Hatté[e], Caroline Gauthier[e], Slobodan B. Marković[f], Mladjen Jovanović[f], Tivadar Gaudenyi[f], Olivier Moine[a], Julien Rossignol[g]

[a]*UMR CNRS 8591, Laboratoire de Géographyie Physique, 1 Place A. Briand, 92 195 Meudon, France*
[b]*Ecole Normale Supérieure, Laboratoire de Météorologie Dynamique & CERES-ERTI, UMR CNRS 8539, 24 rue Lhomond, 75231 Paris Cedex, France*
[c]*Lamont-Doherty Earth Observatory of Columbia University, Palisades, NY 10964, USA*
[d]*Lehrstuhl Geomorphologie, Universität Bayreuth, D-95440 Bayreuth, Germany*
[e]*Laboratoire des Sciences du Climat et de l'Environnement, UMR CNRS CEA 1572, Avenue de la Terrasse, 91198 Gif-sur-Yvette, France*
[f]*Chair of Physical Geography, Faculty of Sciences, University of Novi Sad, Trg Dositeja Obradovica 3, 21000 Novi Sad, Serbia*
[g]*Université de Montpellier II, Institut des Sciences de l'Evolution, UMR CNRS 5554, 34095 Montpellier Cedex 05, France*

Available online 7 January 2009

Abstract

High-resolution study of the Surduk loess palaeosols sequence in Serbia (Vojvodina) has been performed within a research project (EOLE) focusing on the impact of rapid climatic changes during the last climatic cycle in the European loess belt. The methodology used for this multidisciplinary approach is based on a continuous sampling column that allows a very accurate correlation between all studied proxies (magnetic susceptibility, grain size and organic carbon) and the dated samples (IRSL, ^{14}C). According to the stratigraphical and sedimentological data, the Surduk loess sequence appears as a very complete record of the last climatic cycle (19 m), and exhibits a similar pattern than other contemporaneous loess sequences from Western, Central and Eastern Europe. The main difference is the evidence of a drier environment all over the last climatic cycle (sedimentological and palaeopedological data). The high-resolution grain size record (5 cm) is well correlated with stratigraphical boundaries, and highlights a strong variability within the loess deposition, especially during the Upper Pleniglacial between ca. 33 and 15 ka. During the Upper Pleniglacial, a succession of millennial-timescale events, characterised by the deposition of coarser loess, are particularly well evidenced by grain size data as in some west-European records. Finally, an attempt to correlate the variations of grain size parameters at Surduk with the Greenland GRIP dust record is proposed. According to this study, millennial-timescale climatic events that characterise the North Atlantic area during the last climatic cycle have thus been recorded in the environments located at the southern border of the European loess belt.

1. Introduction

For considerable time, research has been focused on stratigraphical correlation, palaeopedology, periglacial processes and dating within the European loess belt (e.g. Bronger, 1976; Kukla, 1977; Sommé et al., 1980; Haesaerts, 1985; Lautridou, 1985; Rousseau, 1987; Zöller et al., 1988, 1994, 2004; Antoine et al., 1999, 2003b; Frechen, 1999; Frechen et al., 2003). These investigations have yielded a unified high-resolution stratigraphical framework for the Upper Pleistocene in Western and Central Europe (Antoine et al., 2001, 2003a, 2003b; Haesaerts et al., 2003; Gerasimenko, 2006). Relying on this background, new research focusing on both variability and impact of rapid climatic events and variability on European loess environments during the Last Glacial has been accomplished (e.g. Hatté et al., 1998; Rousseau et al., 1998, 2001, 2002; Vandenberghe et al., 1998; Antoine et al., 2001, 2003a; Moine et al., 2005, 2008).

Following the investigations on grain size variations in Chinese loess (Liu, 1985; Xiao et al., 1995; Vandenberghe et al., 1997; Ding et al., 1998, 2002; Nugteren et al., 2004), grain size records have been obtained from Last Glacial

*Corresponding author. Tel./fax: +33 1 45 07 55 54.
E-mail address: Pierre.Antoine@cnrs-bellevue.fr (P. Antoine).

1040-6182/$ - see front matter © 2009 Elsevier Ltd and INQUA. All rights reserved.
doi:10.1016/j.quaint.2008.12.008

loess sequences in Poland (Dolecki, 1986), in Belgium (Kesselt: Vandenberghe et al., 1998), in Germany (Nussloch: Antoine et al., 2001, 2003a; Rousseau et al., 2002, 2007) and in Czech Republic (Dolni Vestonice: Shi et al., 2003).

In the Serbian part of the Vojvodina region, numerous loess–palaeosol sections have been recently investigated (e.g. Bronger et al., 1985; Bronger, 2003; Marković et al., 2004, 2005, 2006, 2007; Bokhorst et al., 2006, this issue), providing renewed information on Middle and Upper Pleistocene sequences despite the lack of reliable numerical age estimates (Frechen et al., 2003). The first TL dating results supplied by Singhvi et al. (1989) are now completed by new results obtained by Fuchs et al. (2007) and Marković et al. (2007, 2008).

Based on the methodology developed for the study of the Nussloch reference sequence in Germany (Hatté et al., 1998; Antoine et al., 2001, 2003a; Rousseau et al., 2002; Lang et al., 2003) (EOLE Project), high-resolution multi-proxy investigations were proposed for the Surduk loess section (stratigraphy, grain size, organic carbon, ^{14}C and OSL dating) for two reasons:

1 The location of this section at the southern edge of the European loess belt provides complementary information compared to Northwest and Central European loess records, palaeoenvironnements and wind regimes.
2 According to recent investigations (Markoviæ et al., 2006, 2008), the Surduk section shows one of the best developed record of the last climatic cycle in the area

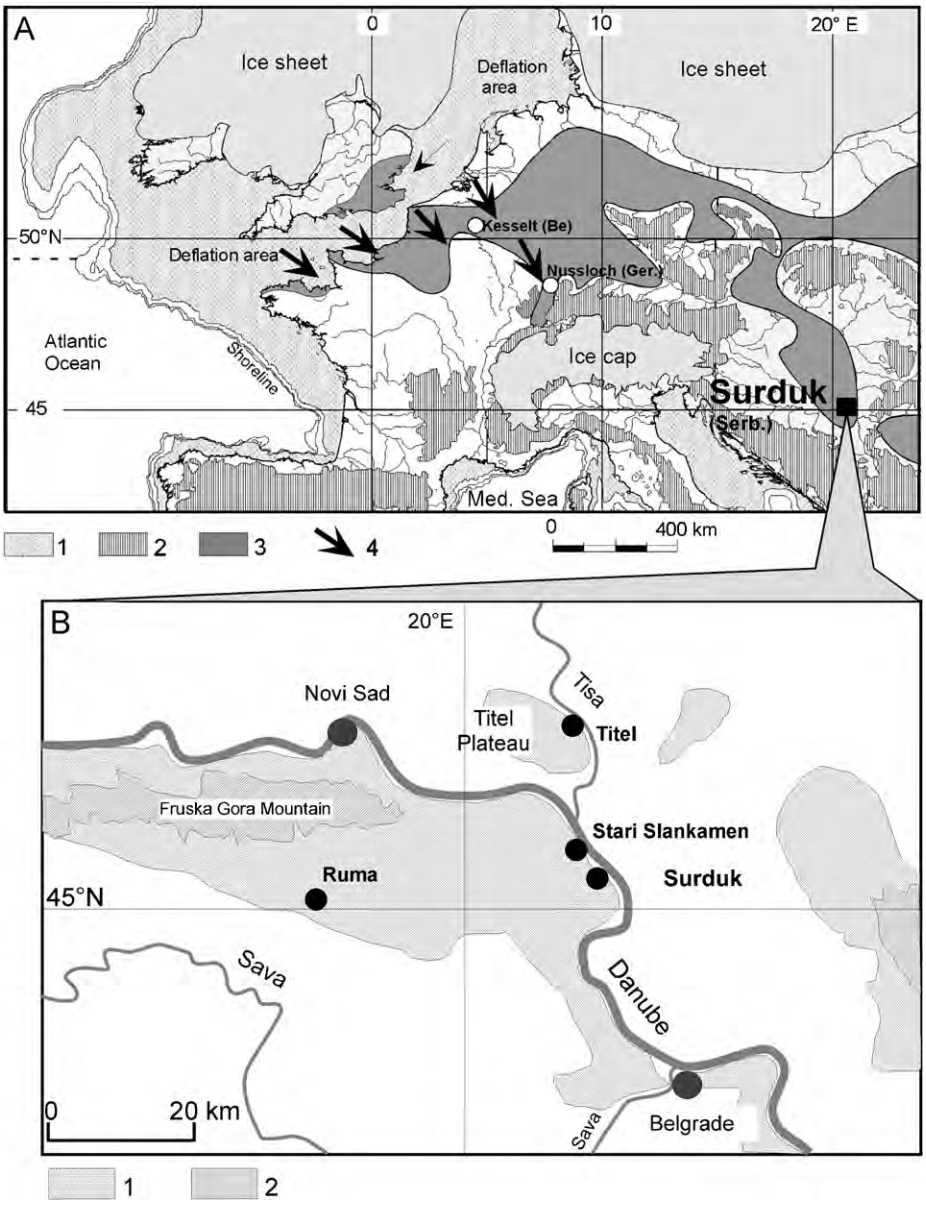

Fig. 1. Location of the Surduk loess section. (A) Location of the Surduk section in a simplified palaeogeographic map of Europe during the LGM: (1) Emerged continental shelf during LGM (deflation area), (2) mountain area, (3) simplified extension of the Last Glacial loess, (4) main wind direction. (B) Location of the Surduk sequence in the Vojvodina region in Serbia: (1) loess and (2) sand (from Marković et al., 2004 modified).

(ca. 19 m), and is thus well suited for the detection of the impact of rapid climatic changes using stratigraphy, sedimentology and geochemistry.

Therefore the aim of this paper is to:

1 Present the results of the multidisciplinary investigations performed on the Surduk section focusing on stratigraphy, grain size, organic carbon and dating.
2 Propose a chronostratigraphical and environmental interpretation of the sequence based on comparisons with regional and other European loess sequences.
3 Suggest a comparison between variations in the loess grain size at Surduk and dust records from Greenland ice cores based on the methodology developed for west-European loess series (Rousseau et al., 2002, 2007; Antoine et al., 2003a).

2. Regional setting and stratigraphy

The Surduk loess section is located on the right bank of the Danube River (45°04′N; 20°20′E, ca. 111 m asl), in the south-eastern part of the Carpathian Basin, ca. 30 km northwest of Belgrade, Serbia (Fig. 1). The section is located at ca. 9 km southeast of the well-known Stari Slankamen profile showing a 40-m-thick loess cliff including 10 fossil soils (Bronger, 1976). The whole area is characterised by the occurrence of thick loess–palaeosol sequences mainly outcropping as high loess cliffs along the western bank of the Danube River, and at the confluence between the Danube and other tributaries, including the Tisa River east of the Titel Plateau.

In previous publications, the prefix "SL" was used to refer to the Stari Slankamen site as a standard section of the region in the stratigraphical labelling scheme (Marković et al., 2003, 2004, 2006). However, to avoid confusion in the loess (L) and palaeosol (S) labelling system, the prefix "V" is used to refer to the standard Pleistocene loess–palaeosol stratigraphy in Vojvodina (Marković et al., 2008).

According to the current chronostratigraphical interpretation (Marković et al., 2004, 2005, 2006) the Last Glacial is represented along the Danube loess cliff, between Stari Slankamen and Surduk, by ca. 8–17 m of typical calcareous loess (V-L1) with a sandy component at the base. In some profiles, it may include a weak organic soil horizon or light brown soil complex (V-L1S1) in its middle part. This entire loess cover is correlated with MIS 4 to 2. It overlies a well-marked Interglacial–Early Glacial soil complex (V-S1) equivalent to fossil soil F2 of Bronger's nomenclature, and correlated with marine oxygen-isotope stage 5.

3. Methodology

3.1. Sampling

Both stratigraphical study and high-resolution sampling were carried out on a 20 m high vertical loess cliff over 15 days (Fig. 2). Due to stability problems, the upper 3 m of the section was sampled in a trench excavated from the top above the vertical profile. The work began with the careful cleaning of the whole section allowing the definition of 14 stratigraphical units.

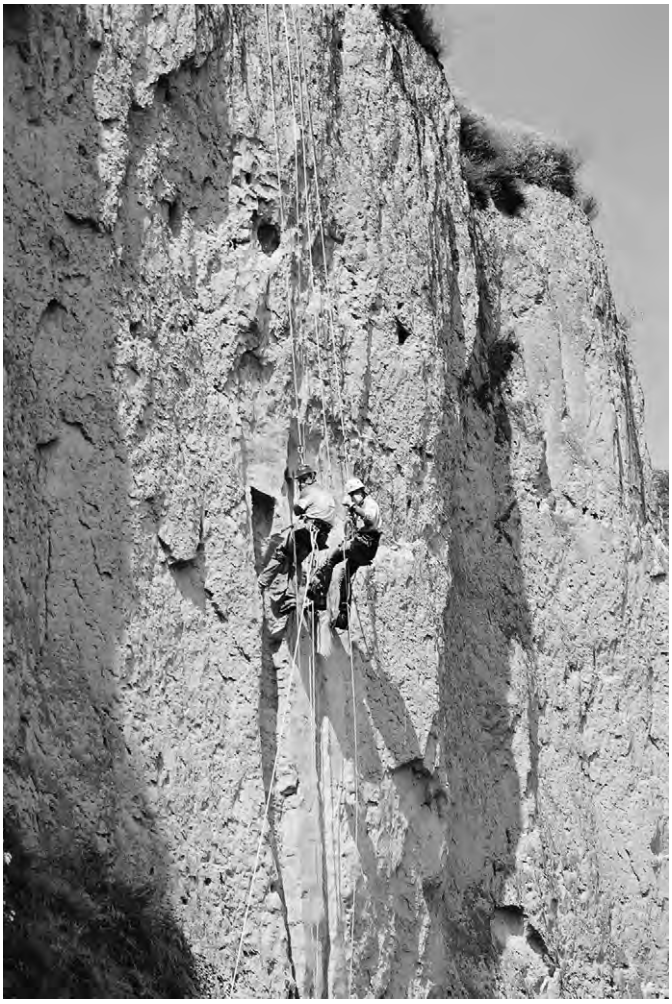

Fig. 2. Continuous sampling on the Surduk loess cliff (Photo S. Marković).

The sampling methodology used at Surduk for grain size and geochemistry was based on the cutting of a vertical continuous loess column (±5–7 cm width), through the whole loess–palaeosol sequence, sliced every 5 cm to produce 376 homogeneous samples of sediment (ca. 300 g; Fig. 3). This continuous column sampling (CCS) method allows averaging the grain size signal every 5 cm, preventing any gap between the various samples, which usually occurs using a succession of isolated samples. During fieldwork, sub-samples (ca. 50 g) were extracted from the previous samples for total organic carbon (TOC) measurement.

3.2. Grain size

Particle size distributions were determined using a Beckman-Coulter LS-230 Laser Particle Sizer (LPS), from

10-g homogenised sub-samples dispersed by sodium hexametaphosphate (0.5%) during 2 h in a rotating agitator (400 ml/10 g), and then sieved at 160 μm to remove the coarse fraction (coarse sands, $CaCO_3$ and FeMn concretions, calcified rootlets, mollusc shell fragments, etc.). Two samples were obtained by direct "pipetting" to obtain a saturation value between 8% and 12% for the PIDS (difference in diffusion of the polarised intensity) and between 45% and 55% for the whole sensors. The measurements were repeated at least three times in order to check the precision of the values.

Calibration of the results provided by the LPS was achieved by applying both LPS and classical analysis on a set of 7 test samples originating from well-contrasted loess and soil facies (Table 1). This comparison shows that the classical cuts at 2, 20 and 50 μm, used with the sieve and pipette method, correspond respectively to ca. 4.6, 22.73 and 63 μm for the Surduk samples analysed with the LPS, as previously proposed by Antoine et al. (2003a), from the Nussloch sequence, and in agreement with published observations (e.g. Konert and Vandenberghe, 1997).

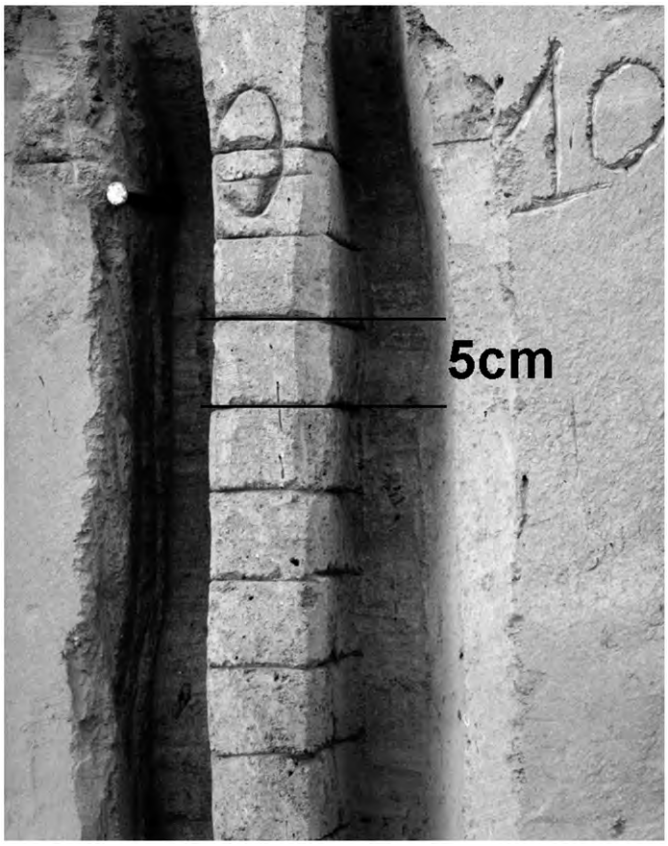

Fig. 3. Continuous Column Sampling method (CCS) used for grain size and geochemistry (Photo P. Antoine).

According to the previous calibration of the LPS results and after numerous tests the best indicator to describe the variations of the grain size along the section was defined as the ratio between coarse loam (22.73–63 μm %), and fine loam and clay (<22.73 μm %). This ratio, named GSI for Grain Size Index appears to be very close to the U-Ratio (44–63 μm/16–44 μm), defined by Vandenberghe et al. (1998).

3.3. Magnetic susceptibility

Magnetic susceptibility was measured using a portable Bartington MF susceptibility meter in parallel with the CCS. After careful cleaning of the section, the susceptibility was measured every 10 cm in loess units and every 5 cm in palaeosols. An average value was calculated from 10 readings per depth.

3.4. Total organic carbon content

The total organic carbon content was determined using an Elementary Analyzer (EA—Carlo Erba NA1500) on 0.6 N HCl leached samples. The complete protocol is presented in Gauthier and Hatté (2007).

3.5. Dating

Ten samples were taken for infrared stimulated luminescence dating (IR-OSL) using cupper cylinders (∅ 4 cm), which were hammered into the loess section to avoid any contamination of the samples with light-exposed material. Additional material was taken from the 30 cm surrounding every IRSL samples for dose rate determination. Sample preparation of the polymineral fine grain fraction (4–11 μm), luminescence measurements and dose rate determination are explained in detail in Fuchs et al. (2007).

Table 1
Grain size results obtained by the classical method (sieve and pipette) on 7 test samples.

Sample (Depth: cm)	Clay (<2 μm %)	Fine silt (2–20 μm %)	Coarse silt (20–50 μm %)	Fine sand (50–200 μm %)	Coarse sands (200–2000 μm %)
17.45–17.50	32.8	27	31.4	8.6	0.2
14.50–14.55	9	21.2	49.7	19.8	0.3
10.65–10.70	19.8	24.5	39.4	15.8	0.5
8.45–8.50	17.1	22.8	42.6	17.4	0.1
8.15–8.20	11	17.5	46.5	24.9	0.1
6.40–6.45	7.2	16	50.4	26.3	0.1
2.55–2.60	13.6	28.9	45.7	11.6	0.2

Amongst sediment sampled for organic geochemistry, some were sub-sampled for ^{14}C dating by AMS on loess organic carbon, according to Hatté et al. (2001). Dating was still in progress at the time of writing, and results are now available at 5.2, 6.65 and 8.35 m depth below the surface. Radiocarbon age estimates are older than 20 ka, out of the calibration range. They are corrected (corr.) according to Bard's equation (Bard, 1998; Bard et al., 1998).

4. Results

4.1. Stratigraphy

During field work, 14 sedimentary and pedological units were identified along the 20-m-thick loess profile (Fig. 4). These units are described from top to base:

1—Dark brown humic silt with irregular bioturbated lower boundary including ceramic fragments at the base (reworked Ah horizon of Chernozem/top soil).
1/2—Calcareous loess with numerous bioturbations and root tracks originating from overlying soil horizon
2—Pale yellow to light brown calcareous porous loess with some root tracks at the top.
3—Light brow calcareous loess with granular porous structure aggregates (''crunchy loess''), and a few earthworm or insects casts.
4—Grey-brown humic silt with granular structure, numerous bioturbations and root tracks, strongly bioturbated upper and lower boundaries (Ah horizon of ''steppe soil'', locally named Surduk soil).
5—Light grey-brown sandy loess with granular structure.
6—Grey-brown sandy loess with granular structure (weakly developed humic soil horizon).
7—Light brown sandy silt with strong granular structure (2–4 mm), numerous earthworms and insects casts in the middle part (∅ 0.5–1 cm). Numerous FeMn nodules coatings on root tracks (weakly developed Bw horizon, of Cambisol).
8—Light yellow grey sandy loess with some sandy layers (⩽5 mm).
9—Light brown grey massive sandy loess with numerous rootlets tracks (∅ ⩽1 mm) scattered little FeMn nodules (weakly developed Bw horizon, of Cambisol).
10a—Light grey to light brown laminated sandy loess with numerous sand layers (up to 5 mm) and some thin lenses of reworked soil aggregates.
10b—Light grey to light brown sandy loess with numerous sand layers.
11—Massive homogeneous grey-brown silt with numerous FeMn nodules (⩽1 mm) and FeMn coatings around rootlets tracks.
12—Brown to brown grey non-calcareous dense and homogeneous humic silt with granular structure, rootlets track and bioturbated boundaries (Ah horizon of Chernozem soil).
13b—Very dense, non-calcareous brown clayey silt with diffuse prismatic structure, numerous rootlets tracks and earthworm bioturbations (burrow and hibernation casts) (Bth horizon of Luvic Chernozem).
13a–b—Lightly more greyish horizon observed between 13a and 13b (diffuse boundaries).
13a—Very dense, non-calcareous dark brown clayey silt with granular structure numerous rootlets tracks and earthworm bioturbations (burrow and hibernation casts) (Bth horizon of Luvic Chernozem, FAO, 2006). Strongly irregular lower boundary with large bioturbations and root tracks).
14—Yellow and homogeneous calcareous loess with large calcareous nodules (''loess dolls'', up to 10 cm in diameter) and mollusc shells. Only the top 1 m of this loess unit is exposed.

4.2. Magnetic susceptibility

The magnetic susceptibility (MS) record shows values varying between ca. 10 in the loess deposits and ca. 91 SI units in the lower soil complex (Fig. 4). Loess unit 14 shows low values of ca. 11 SI units, which strongly increase to reach the highest values at the top of subunit 13a. Subunits 13a/b and 13b show a three-step decrease in MS values with plateaus at ca. 84, 75 and 59 SI units. Unit 12 corresponds to another decreasing step to ca. 36 SI units, and unit 11 corresponds to the last decreasing step toward the lowest values (ca. 19 SI units). MS in the first loess layers (units 10 to 5) is low, especially in the basal sandy unit (minimum of 14.4 SI units). The Surduk soil (unit 4) shows slightly higher values (ca. 23 SI units), but nevertheless much lower than in the lower soil complex or in the topsoil. The Upper loess, units 3 to 2, yields the lowest values (ca. 10 SI units) with an increasing trend toward the top of the series due to contamination from the surface horizon. This increasing trend continues in the topsoil to reach ca. 63 SI units in the uppermost layer, which remains lower than in the lower soil complex likely owing to modern erosion and reworking of the upper part of this soil.

4.3. Total organic carbon

The total organic carbon record can be divided in five parts showing very good agreement with the main stratigraphical boundaries.

The base of the profile shows a rapid enrichment in COT from the top of the loess unit 14 into the lower soil complex. Values vary from 0.1% in loess to a maximum of 0.5% in unit 13b, in agreement with its pedological facies (Luvic Chernozem). The values decrease to the top of the lower soil complex in unit 12, where the pedological development is less marked. Minimum values (<0.1%) are then recorded within the sandy loess unit 10 corresponding to the beginning of pure loess sedimentation.

Enrichment is observed in the soil horizons of the Middle soil complex, as in unit 7 (0.35%) and in unit 4 (Surduk soil) showing a peak value of 0.48%.

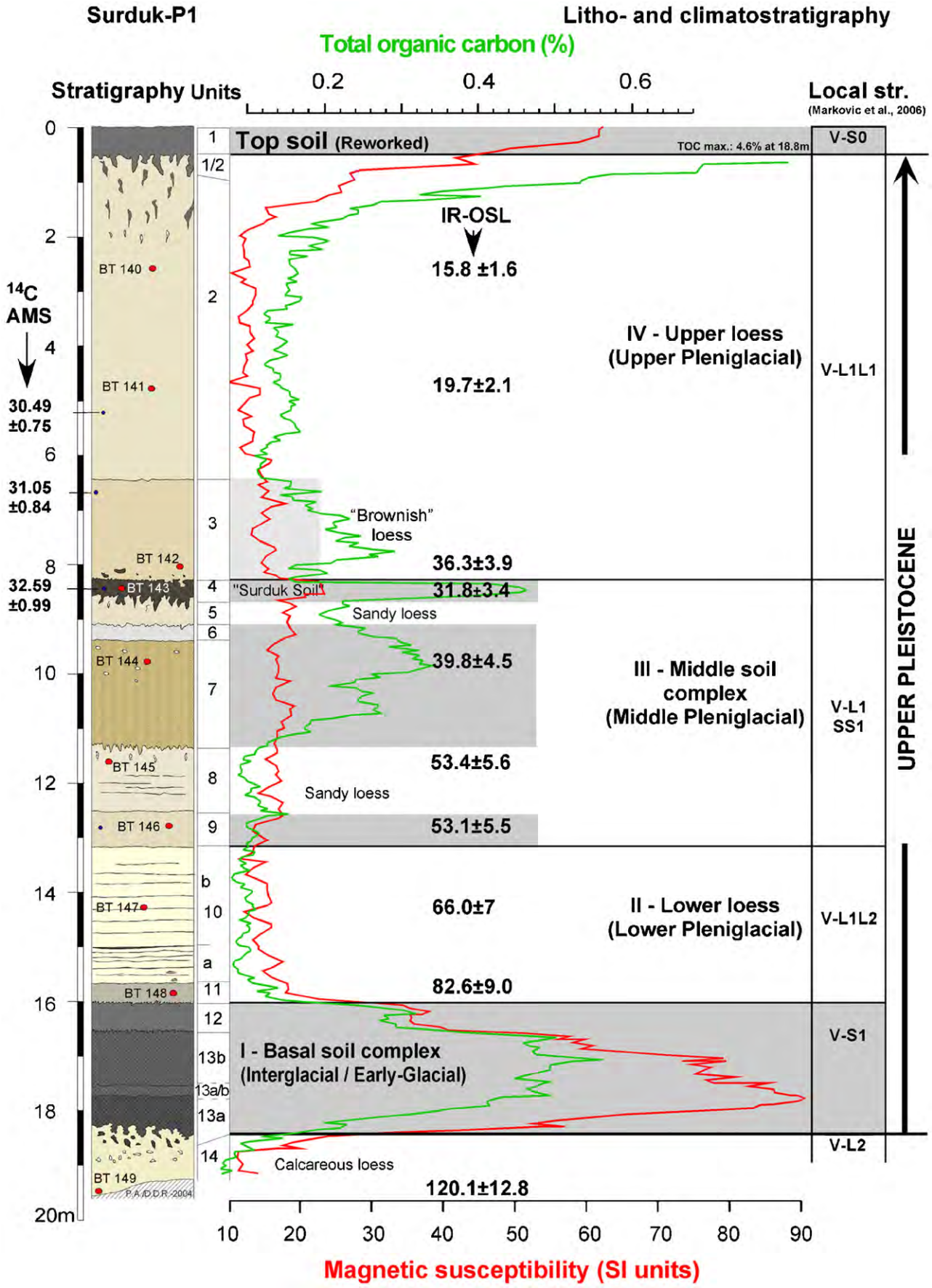

Fig. 4. Stratigraphy, dating, low field magnetic susceptibility and TOC records of the Surduk loess and palaeosols sequence. IR-OSL results according to Fuchs et al. (2007).

A sharp decrease characterises the last loess units (3 and 2) showing low values (average value: ±0.15% between −2 and −8 m). The brownish loess unit indicating more intense biological activity is underlined by a slightly higher COT percentage (0.2–0.3%) compared with the Upper loess unit. The upper 1 m of the last loess deposition is characterised by a progressive enrichment in COT from 0.2% to 0.7% in parallel with an increase in the density of bioturbation (root tracks). The reworked topsoil shows high values up to 4.6%. COT results reinforce the pedological differentiation between the various soil horizons within the profile. Indeed the Luvic Chernozem horizons (Basal soil complex), the brown soils horizons of the Middle soil complex, and especially the Surduk soil are characterised by markedly higher COT values.

4.4. Dating

IR-OSL dating results, including analytical data, are listed in Table 2 and plotted in their stratigraphical position in Fig. 4. Results are discussed in detail in Fuchs et al. (2007). Age values range from 15.8±1.6 ka in the upper part of the section to 120.7±12.8 ka at the base.

Sample BT-149 taken from unit 14 provided an age of 120.7±12.8 ka, which is in agreement with an expected penultimate climatic cycle age (Upper Saalian/MIS 6). The sandy loess of unit 10 yields an age of 66.0±7.0 ka (BT-147), but sedimentation of this lower sandy loess starts at 82.6±9.0 ka (BT-148) with unit 11, directly overlying the upper unit of the lower soil complex.

Four IR-OSL ages were obtained from unit 9 to 4, including the top of the underlying sandy loess and the interstadial soil complex. Two samples with ages of 53.1±5.5 ka (BT 146) in the lowermost incipient soil (unit 9) and 53.4±5.6 ka (BT-145) in the sandy loess of unit 8 are followed by the uppermost sample (BT-144) from the weak brown soil of unit 7, which yielded an age of 39.8±4.5 ka. Dating of the sediment from the humic Surduk soil (unit 4) yielded an age of 31.8±3.4 ka (BT-143).

Three IR-OSL ages have been determined from units 2 and 3. Sample BT-142 extracted from the base of loess unit 3 indicates an age of 36.3±3.9 ka. At 4.9 m depth, sample BT-141 with an age of 19.7±2.1 ka is associated with the onset of pronounced loess accumulation. The uppermost sample BT-140, located at 2.6 m depth in unit 2, yields an age of 15.8±1.6 ka.

The geochronological approach is completed by three AMS radiocarbon age estimates. They have been obtained by AMS dating of loess organic matter from the Upper loess units (units 2 and 3) and from the Surduk soil horizon (Table 3). Taking into account the error bars, the results are in relatively good agreement with stratigraphical order (Fig. 4). They indicate that the deposition of the lower half of the Upper loess sequence occurred around 30 ka and that the Surduk soil has formed around 32 ka.

4.5. Grain size

The cumulative grain size curves from nine samples, typical of the main stratigraphical units, are presented in Fig. 5. According to the differences in the shapes of their curves, samples were grouped in three categories.

A first category illustrated by the curves of samples 17.50–17.55 and 17.20–17.25 m extracted from the Bth horizon (unit 13a) is characterised by the juxtaposition of

Table 3
AMS radiocarbon dating results.

Sample identification			^{14}C age (ka)		^{14}C cor. age[a] (ka)	
Depth (m/top)	GifA[b]	ANUA[c]	Age	±1σ	Mean	±2σ
5.20	50013	31419	26.00	0.33	30.49	0.75
6.65	50014	31420	26.50	0.37	31.05	0.84
8.35	50016	31423	27.87	0.44	32.59	0.99

[a]Corrected according to Bard's equation (Bard et al., 1998).
[b]Chemistry reference.
[c]Physical measurement reference.

Table 2
IR-OSL dating results (according to Fuchs et al., 2007).

Sample	Depth (m)	Δ	a-value	U (μm/g)	Th (μm/g)	K (%)	$\dot{D}$ (Gy/ka)	D_E (Gy)	IR-OSL age (ka)
BT 140	2.60	1.15±0.1	0.05	3.05±0.09	9.77±0.46	1.41±0.03	3.20±0.32	50.41±1.26	15.8±1.6
BT 141	4.90	1.15±0.1	0.10	3.36±0.10	10.83±0.49	1.44±0.03	3.95±0.42	77.80±1.99	19.7±2.1
BT 142	8.00	1.15±0.1	0.08	3.52±0.10	11.79±0.52	1.57±0.03	4.00±0.42	145.19±2.22	36.3±3.9
BT 143	8.40	1.15±0.1	0.05	3.49±0.09	12.50±0.52	1.58±0.03	3.70±0.38	117.49±3.91	31.8±3.4
BT 144	9.80	1.15±0.1	0.07	3.67±0.11	12.34±0.55	1.61±0.04	4.06±0.43	161.56±6.44	39.8±4.5
BT 145	11.60	1.15±0.1	0.06	3.19±0.07	11.09±0.40	1.57±0.03	3.57±0.37	190.60±2.85	53.4±5.6
BT 146	12.70	1.15±0.1	0.06	3.12±0.10	11.13±0.53	1.58±0.04	3.56±0.37	188.80±1.44	53.1±5.5
BT 147	14.20	1.15±0.1	0.06	3.38±0.09	11.59±0.49	1.67±0.03	3.76±0.39	247.90±3.78	66.0±7.0
BT 148	15.80	1.15±0.1	0.06	3.53±0.10	12.25±0.54	1.70±0.03	3.89±0.41	321.46±9.76	82.6±9.0
BT 149	19.40	1.15±0.1	0.06	2.99±0.11	10.49±0.56	1.38±0.04	3.25±0.34	391.90±4.77	120.7±12.8

Note: Δ = water content given as the ratio of wet sample weight to dry sample weight; a-value = α-efficiency factor; U-, Th-, and K-concentrations based on low-level γ-spectrometry (in none of the samples significant radioactive disequilibrium was present); U-concentrations calculated from ^{214}Bi and ^{214}Pb activities; $\dot{D}$ = effective dose rate; D_E = equivalent dose.

three well-individualised populations of grains: fine clay between ca. 0.1 and 1 μm, "coarse" clay and fine loam between 1 and 10 μm and a more marked fine-to-coarse loam between ca. 10 and 60 μm.

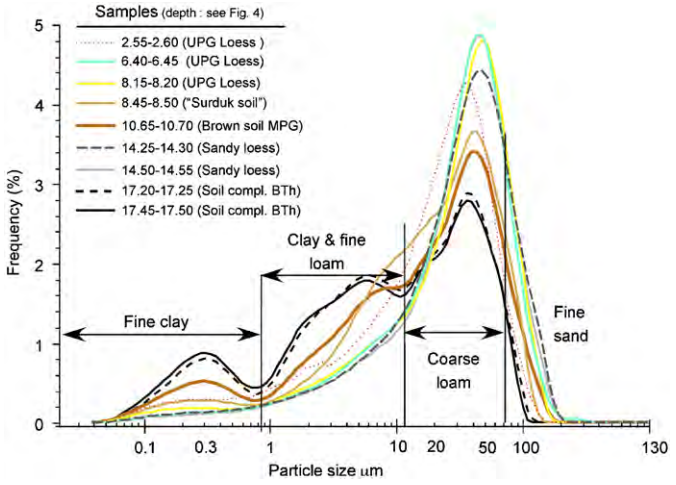

Fig. 5. Cumulative grain size curves from the main stratigraphical units of the Surduk section (Beckman-Coulter LS-230 Laser Particle Sizer).

The second category is illustrated by the curve of sample 10.65–10.70 m (unit 7, "brown soil"), which also shows three main populations but less pronounced fine clay and fine loam components. The curve determined for the Surduk soil sample (8.45–8.50 m) has an intermediate shape between categories 1 and 2 with a very low fine clay component but enrichment in fine loam between 10 and 20 μm.

The third category is illustrated by three samples originating from the Upper loess (8.15–8.20, 6.40–6.45, 2.55–2.60). The sorting of the particles is particularly good and characterised by a narrow and regular Gauss curve with a marked maximum around 40–50 μm in the coarse loam, as generally observed in typical Upper Pleistocene loess. The two samples from the sandy loess unit 10a (14.50–14.55 and 14.25–14.30 m) show the same "loessic" pattern, except a shift of their curve maxima between 100 and 110 μm.

In the first category, the strong enrichment in fine clay (illuviation) characterising the Bth horizons of the lower soil complex (up to 35%) is coupled with illuviation of clay particles (coarser than 1 μm) and in fine loam (1–10 μm), typical of soils formed under continental climates as grey

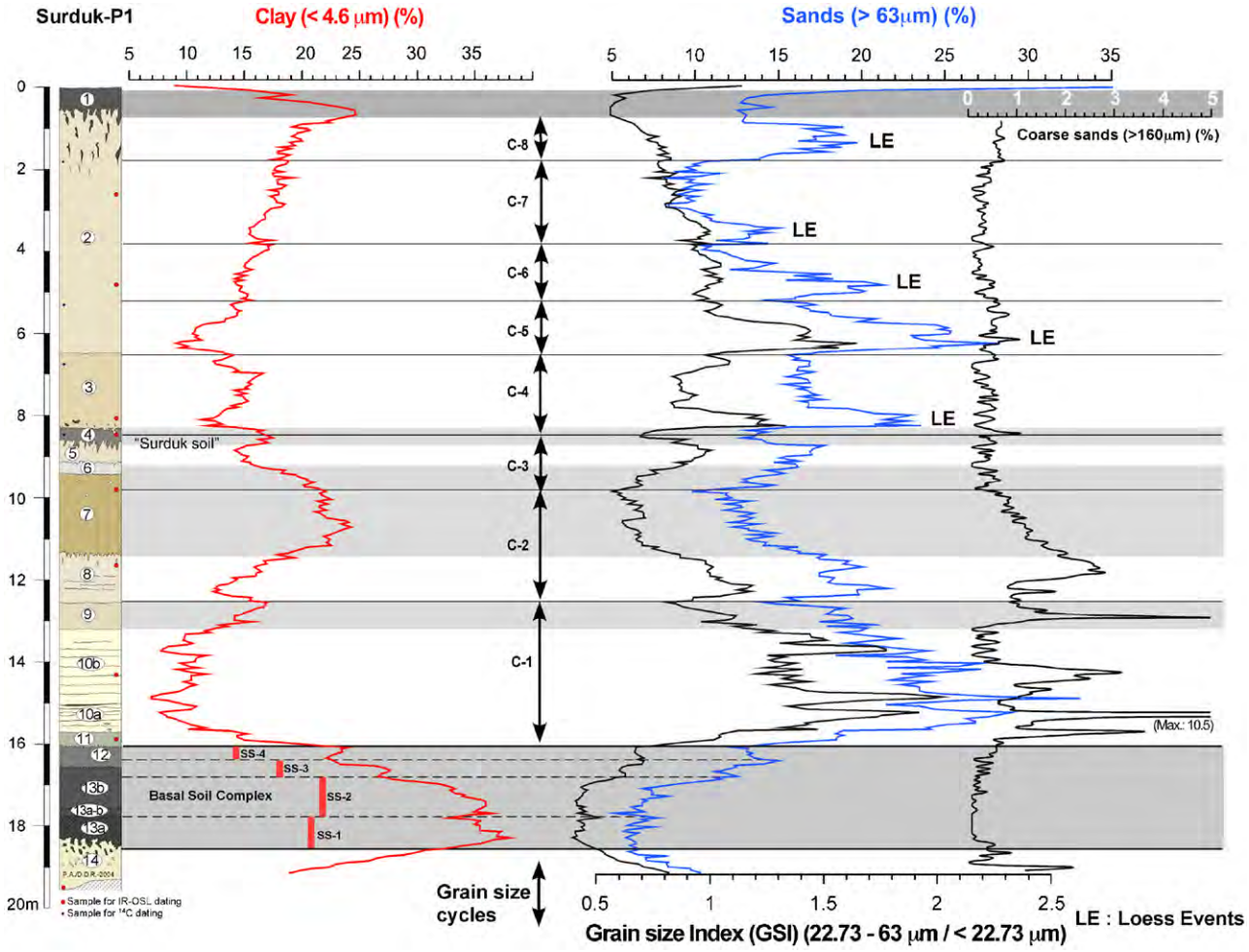

Fig. 6. Variation of the grain size parameters compared to stratigraphy; definition of grain size cycles (C) and of Loess Events (LE).

forest soils or leached Chernozems (Van Vliet-Lanoë, 1987; Antoine et al., 2003b). In these soils, the melting of the snow cover in Spring induces a leaching of surface particles down the profile using biological voids (earthworm burrows) and desiccation cracks. In thin sections, these processes are underlined by the presence of thick-laminated argillans formed by the alternation of humic clay and of silty bands (Antoine et al., 2003b).

According to grain size data, the pedological processes involved in the formation of the brown soil horizons of unit 7 and of the humic horizon of the Surduk soil, are clearly different as the fine clay and silt illuviation processes are weaker or even absent, as in the Surduk soil horizon mainly individualised by a higher amount of TOC.

Comparison with pedo-stratigraphical data thus shows that these strong differences in the shape of the cumulative grain size curves are mainly related to the relative impacts of the pedological processes rather than to variations in the source of loessic material.

4.6. Continuous high-resolution record

The results of the grain size analysis yields a continuous high-resolution record of the grain size variations along the 19.2-m-thick sequence. Comparison between the continuous records of grain size parameters and the stratigraphical sequence shows a very good agreement (Fig. 6). The main stratigraphical boundaries, as for example those between the lower soil complex and the Surduk soil, and their respective overlying loesses, are recorded by abrupt variations in the grains size parameters without any vertical drift.

The main grain size variations and contrasts are observed in the clay ($<4.6\,\mu m$: from 10% to 35%), in the coarse silt (22.73–63 μm: from 7% to more than 25%) and in the fine sand ($>63\,\mu m$: from 0% to 5%) percentages. In addition, the Grain Size Index (GSI) (ratio between coarse silt/fine silt plus clay) shows contrasting grain size patterns, especially within the Upper loess deposits (units 3 and 2).

5. Chronoclimatic interpretation and stratigraphic correlations

Above the basal loess layer (L2), allocated to the penultimate cold phase, i.e. Upper Saalian (MIS 6) in agreement with an IR-OSL age of 120.7 ± 12.8 ka, a subdivision of the Surduk section into four main chronoclimatic sequences is proposed, taking into account the observations, analytical data and geochronological results (Fig. 4).

5.1. Sequence I: Basal soil complex

The first sequence includes the thick humic and clayey lower soil complex (units 13 and 12). The main part of this complex (unit 13) is composed of two superimposed Bth horizons of leached Chernozem soils (Luvic Chernozem) characterised by very high clay (26–35%) and TOC (0.4–0.6%) percentages. The distinction between these two horizons is not obvious *in situ*, with only a slight difference in colour. It is nevertheless reinforced by the clay data showing two maxima (35% and 37%) separated by a relative decrease at the top of 13a (Fig. 6).

In addition, the occurrence of the highest MS values within the main humic and clayey soil horizons of the Basal soil complex suggests that the enrichment in magnetic minerals responsible for high MS values is linked to pedological processes, as proposed from Chinese loess (Heller and Evans, 1995; Sun and Huang, 2006), or to organic pedogenesis in the case of European loess sequences (Rousseau et al., 1998; Antoine et al., 1999, 2003b). This pedological enrichment in magnetic minerals (magnetite and maghemite) has been attributed to bacterial activity (magnetotactic bacteria) within soil horizons (Maher and Taylor, 1988) and can be used as a proxy of palaeoprecipitation (Maher et al., 2003).

The huge peak observed throughout the Basal soil complex in clay and TOC percentages and in MS, and the very low coarse particles ($>160\,\mu m$) percentages slightly increasing at the top of unit 12 (Figs. 4 and 6) support the pedological origin of the fine clay component within these soil horizons. A more detailed analysis of the clay and TOC percentages and of GSI values allows the subdivision of the pedocomplex in four subsequences (SS-1 to SS-4), which are more or less well correlated with the stratigraphical and MS records as shown in Fig. 6.

The boundaries between these sub-cycles rely on minima in both clay and TOC percentages, and maxima in GSI, and are located at the upper boundary of unit 13a, close to the top of unit 13b, and at the upper boundary of unit 13b. Unit 13b thus appears to be divided into two subsequences, SS-2 and SS-3, showing that the succession of pedological events is probably more complex than that deduced from the pedo-stratigraphical approach. Superimposed on these subsequences, the general trend in clay and TOC percentages, and in MS, between the upper half of unit 13a and the top of unit 12 underlines a progressive evolution to more arid conditions and a shift from a continental forest to a steppe-like landscape during the end of the Early Glacial. This evolution is especially rapid during SS-3 (top of unit 13b) and SS-4 (unit 12) and characterised by a synchronous two-step decrease in clay and TOC percentages, and in MS.

According to its pedological facies and relatively low clay content (ca. 20%) compared with the underlying Bth horizons, the dark brown Ah humic horizon (unit 12) shows a steppe soil facies that indicates a first step to more arid and cooler conditions.

The Basal soil complex has been attributed to the Last Interglacial–Early Glacial period (MIS 5) on the basis of its pedological characteristics and of comparisons with other regional and European loess series (Marković et al., 2004, 2005, 2006, 2007). The IR-OSL age obtained from the grey loess overlying the soil complex (82.6 ± 9 ka) supports this

attribution. However, it is not possible to exclude a slight overestimation of the IR-OSL age of unit 11 owing to the probable inclusion of unbleached grains reworked from underlying soil units during its deposition.

Compared with the Ruma section located ca. 40 km to the west (Fig. 1B), the pedosedimentary budget of the 2.3-m-thick Basal soil complex (V-S1) in Surduk appears to be highly condensed. V-S1 is represented in Ruma by a more than 4-m-thick soil complex preserved in a large palaeo-depression. From the top to the base, the Ruma soil complex is composed of at least two steppe soil horizons (Ah), and two thick clayey and humic soil horizons with a prismatic structure (Bth) overlying a clearly distinct brown-orange Bt horizon (Marković et al., 2004). This Last Interglacial–Early Glacial pedosedimentary sequence is very similar to those of Western Europe like Achenheim (Rousseau et al., 1994, 1998), or Saint-Sauflieu in Northern France (Antoine et al., 1999).

Such comparisons show that the climate during the first part of the Last Interglacial was sufficiently humid for the development of (forested) leached soils that have been overprinted by Chernozem pedogenesis during the following interstadials of the Early Glacial in different regions in Europe.

5.2. Sequence II: Lower loess

The second sequence begins with the onset of pure loess sedimentation represented by 0.3 m of grey loess (unit 11) including reworked organic silty particles originating from the upper humic soil layer (unit 12). TOC percentages are close to zero underlining the disappearance of pedological processes. The deposition of this first loess unit including local silty material is followed by the deposition of a 2.8-m-thick calcareous sandy loess showing numerous intercalated sandy layers (2–10 mm, unit 10).

The structure of the sandy layers intercalated within this loess and the absence of erosion gullies show that these layers do not result from hillwash processes; moreover, there is no relief and no evidence of paleorelief allowing hillwash process at that place. Conversely, they likely indicate the periodical occurrence of strong winds able to drift the sand grains from the Danube braided alluvial plain, prevailing during Pleniglacial times. This sandy component, also described in the sections from Titel plateau located 20 km to the North (Bokhorst et al., 2006, this issue; Marković et al., 2008), appears to be characteristic of the Lower loess in the whole area. According to their facies and stratigraphical location within the section, both units 10 and 11 are allocated to the Weichselian Lower Pleniglacial, supported by the IR-OSL age BT-147 (66.0 ± 7 ka) obtained from unit 10b which indicates that the L1L2 loess deposited during MIS 4.

5.3. Sequence III: Middle soil complex

The third sequence begins with the development of a new soil and sandy loess complex, 4.9-m thick (units 9–4). This complex is composed of a succession of weakly developed grey-brown to light brown cambic horizons (units 9 and 7), separated by sandy loess units (units 5 and 8) and toped by a 0.3-m-thick humic horizon, named Surduk soil (unit 4). The apparently weak development of the "brown soils" (units 9 and 7), according to field observation, is nevertheless well marked in the TOC and clay percentages that are much higher than in the loess, especially for unit 9 (Figs. 4 and 6). This alternation of loess deposition and weak development of "brown soils" is similar to those described not only for the Middle Pleniglacial in north-western Europe (e.g. Antoine et al., 1999, 2001; Schirmer, 2000) but also in central and east-European sequences (e.g. Kukla, 1977; Veklitch, 1979; Rousseau et al., 2001).

This Middle soil complex, mainly composed of weakly developed cambisols (units 9 and 7), is not characterised by higher MS values. Only the Surduk soil horizon appears clearly in the MS signal. This last observation reinforces the correlation between MS values and TOC content in the loess record. The Surduk MS record shows similarities with measurements performed in both Dolni Vestonice, in the Czech Republic and Vyazivok in Ukraine (Rousseau et al., 2001). In all these sequences, the main Weichselian Lower and Upper Pleniglacial aeolian deposits show very low MS values that bracket slightly higher ones measured in the Middle soil complexes.

The pedological and sedimentological characteristics of the Middle soil complex at Surduk indicate an important reduction of the global dust flux that is typical of this period in European loess sequences (Antoine et al., 1999; Frechen et al., 2003; Haesaerts et al., 2003). According to IR-OSL and ^{14}C dates, this period lasted from ca. 55 to 32 ka. There is good agreement between luminescence dating (31.8 ± 3.4 ka) and radiocarbon AMS result on loess organic matter (32.59 ± 0.9 corr. ka) for the Surduk soil (Fig. 4).

5.4. Sequence IV: Upper loess

The fourth sequence is composed of the upper 8 m of the profile, represented by typical loess deposits allocated to the Weichselian Upper Pleniglacial according to their facies, stratigraphical location and geochronological results. This sequence can be divided into two parts:

A lower "brownish loess" (2 m), with numerous bioturbations and a relatively high TOC values, indicating a more intense biological activity (unit 3). This unit provided one IR-OSL age of 36.3 ± 3.9 ka at its base and a radiocarbon age of 31.05 ± 0.84 corr. ka in its upper part. Even if it is likely that the sedimentation rate has been lower during the deposition of this brownish loess according to its relatively high clay and TOC percentages, an overestimation of IR-OSL age BT 142 by a few ka is likely. The radiocarbon age obtained ca. 1.2 m upper in unit 3 is definitely younger (31.05 ± 0.84 ka). Taking into account the location of the sample a few centimetres above the Surduk soil, this overestimation could result from an incomplete bleaching

of some grains locally transported as soil aggregates from underlying horizons.

An upper light brown loess (6 m), showing a more homogeneous facies and a few bioturbations (unit 2). This unit has been deposited between about 20 and 15 ka BP according to IR-OSL samples BT-141 and 140.

During the deposition of the Upper loess the accumulation rate increases sharply to values of ca. 0.6 mm/a from BT-142 to BT-141. However, the effective sedimentation rate may have been strongly higher or lower depending on the prevailing process, either loess deposition or soil formation, respectively.

The highest sedimentation rates are thus obtained for the Upper Pleniglacial in agreement with the general pattern described for European series (Frechen et al., 2003, Antoine et al., 2001), and corresponding to the interval during which the Greenland atmosphere was the dustiest (GRIP Members, 1993; NGRIP Members, 2004).

The comparison of AMS and IR-OSL results from unit 2 shows a clear discrepancy around 4.5 m between ^{14}C (30.49 ± 0.7 corr. ka) and IR-OSL (19.7 ± 2.1 ka) obtained about 50 cm above. IR-OSL dating can be underestimated because of a potential bleaching, due to coarse grains. However, ^{14}C dating can be overestimated by incorporation of older organic carbon before the fossilisation step, resulting of an incomplete oxidation, during dust transportation, of original organic matter associated to the mineral grain. Stratigraphical interpretation favours a young age but does not lead to a more proximal origin of the grains for this part of the loess sequence than for the others parts. Progresses in ^{14}C chronology acquisition might solve this issue.

5.5. Top soil

The section is topped by a Chernozem soil horizon (unit 1), characterised by the highest COT percentages and the second highest MS peak of the whole sequence. This horizon, attributed to the Holocene interglacial, is separated from the underlying loess by a strongly bioturbated boundary showing large burrows. However, the discovery of ceramic fragments in unit 1 during the digging of the trench at the top of the section shows that this soil horizon has been strongly eroded and reworked by human activities such as ploughing.

6. Summary and comparisons

Overlying a well-developed Interglacial–Early Glacial clayey-humic soil complex, the 16-m-thick Surduk loess sequence is thus composed of two main periods of loess deposition (units 10 and 2/3) separated by a weakly developed interstadial soil complex attributed to the Middle Pleniglacial (units 9–4).

Such a pedo-stratigraphical pattern is typical of the sequences from the last climatic cycle in Western, Central and Eastern Europe: Saint-Acheul Complex (Antoine et al., 1999), Remagen Complex (Schirmer, 2000), Gräselberg and Lohne soils (Bibus, 1980, Zöller et al., 1988; Semmel, 1997), Stillfried B or PKII complexes (Kukla, 1977), Vytachiv complex (Veklitch, 1979; Rousseau et al., 2001; Gerasimenko, 2006) (Fig. 7). The Surduk record exhibits a general structure that appears very close to that of the other European sequences, which shows that loess records represent very good references for the study of the impact of climate changes over Europe at least during the last climatic cycle.

Compared to Western European loess sequences, the Serbian loess at Surduk exhibits nevertheless some differences in the loess and soil facies, indicating that the environment was definitely drier in the southern Carpathian Basin during the whole last climatic cycle (Fig. 7):

1 Presence of thin aeolian sand beds originating from the Danube alluvial plain within the Lower Pleniglacial loess (unit, 10).
2 Absence of tundra gley layers, frost wedges or ice wedges casts in the whole sequence.
3 Absence of laminated loess facies during the Upper Pleniglacial.
4 Weak development of the Middle Pleniglacial soil horizons.
5 Occurrence of mainly humic pedogenesis during the Interglacial–Early Glacial period and at the end of the Middle Pleniglacial.

6.1. Evidence of cyclic variations during the deposition of Last Glacial loess

High-resolution grain size record, and especially the GSI and >63 μm curves, allow the definition of grain size cycles along the Surduk profile. These cycles are defined following the methodology proposed for the interpretation of the grain size records of the Nussloch reference sequence, where each cycle is defined by the evolution of the grain size parameters from a minimum to a maximum then to a new minimum, drawing generally an asymmetrical pattern (Antoine et al., 2003a; Antoine et al., submitted). The lower boundary of every cycle is underlined by a rapid shift in the various grain size parameters and especially in the GSI and fine sand percentages (Fig. 6).

Above the main stratigraphical boundary between units 11 and 10, the grain size records of the Last Glacial loess from units 10 to 2 allow recognition of a succession of 8 cycles whose thickness varies from 1.5 to 3 m (Fig. 6).

This approach, based on grain size, is completed by a comparison with the variations in TOC percentage reinforcing the opposition between periods of pure loess deposition (low TOC percentage, high GSI and fine sand percentages) and periods of pedogenesis (high TOC percentage and low GSI and fine sand percentage). GSI and especially the coarse particle record allow the definition of a succession of short events of coarse loess

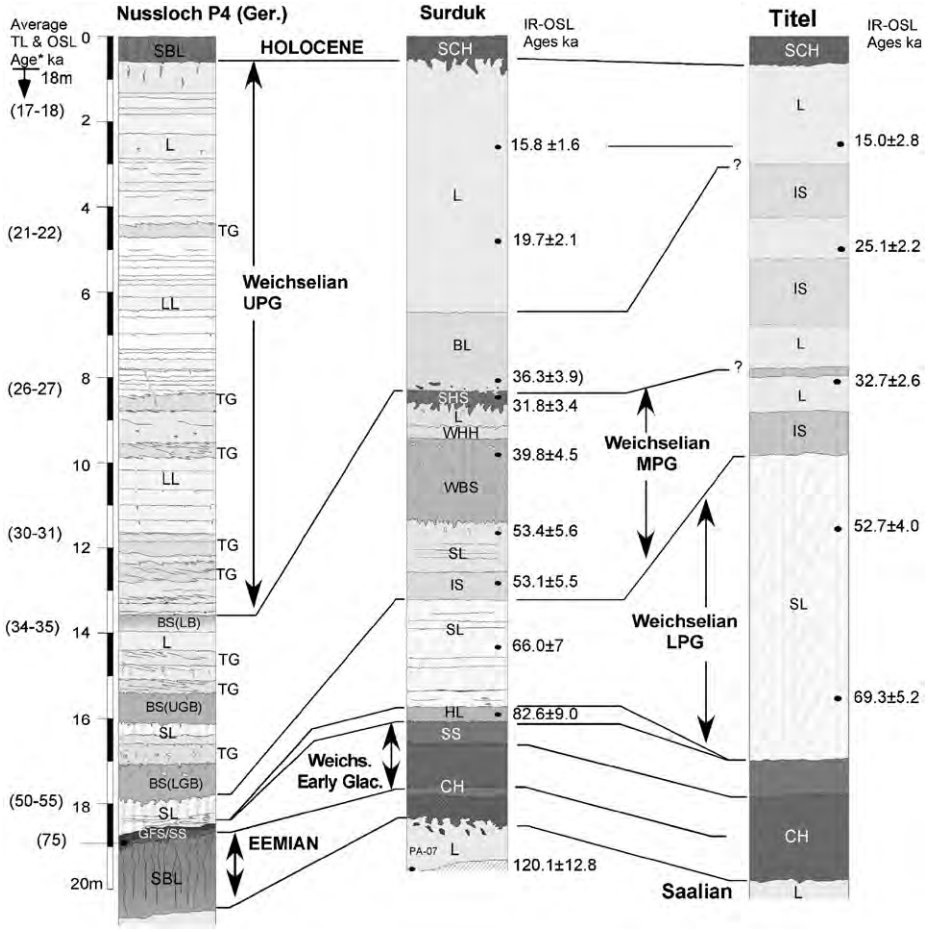

Fig. 7. Stratigraphical correlation between the sequences of Surduk, Titel and Nussloch. Abbreviations: *Soils*: CH-Bth Hz. of Luvic Chernozem, SCH: surface Chernozem Hz., SBL: Bt Hz. of Luvisol SS-Steppe soil horizon (Ah) GFS-Bth Hz. of grey forest soil BS-Bw Hz. of arctic brown soil (LGB: lower Gräselberg Boden, UGB: Upper Gräselberg Boden, LB: Lohner Boden), WBS—weakly developed brown soil horizon, IS—incipient (brown) soil Hz., SHS—Surduk humic Hz., WHH—weakly developed humic horizon, TG—Tundra gley Hz. *Sediments*: L—loess (homogeneous), SL—sandy loess, LL—laminated loess, BL—Brownish "crunchy" loess.

deposition called "Loess Events" (LE) within the apparently homogeneous loess units of the Upper Pleniglacial (units 3 and 2).

6.1.1. Cycle 1 (thickness: ca. 3.2 m)

The first grain size cycle starts with the onset of Pleniglacial sedimentation corresponding to loess units 11, 10a and 10b and ends with the weak brown soil of unit 9. The lower boundary corresponds to a rapid shift in all the grain size parameters at the basis of the first calcareous loess. This shift is marked by a rapid decrease in the clay percentages (from 20% to 10%) and in TOC downward to 0.1% at the top of unit 11. Unit 10 is then characterised by stable and very low values in clay (ca. 10%) and in TOC (0.1%), typical of Pleniglacial conditions. Conversely, GSI fine sand and coarse particle percentages show a very rapid rise at the base of unit 10a followed by a succession of short maximums. This strongly asymmetrical grain size cycle ends by a progressive decrease in all the coarse grain components and a slight enrichment in clay in the weakly developed soil 9, showing the reduction in the aeolian dynamics and a relative increase in pedological processes.

6.1.2. Cycle 2 (thickness: ca. 2.8 m)

Cycle 2 includes unit 8 and most of unit 7. Grain size parameter curves show an asymmetrical trend with a rapid rise in the coarse grain components at the base of unit 8 (including a double peak) followed by a progressive decrease within unit 7.

The variations in clay and TOC percentages are roughly parallel, and show a progressive increase up to a maximum in the upper part of soil unit 7 (TOC: 0.3%, clay: 22–25%). The evolution of the grain size parameters shows a rapid decrease in the clay percentage starting ca. 30 cm below the stratigraphical boundary (7/6). This observation indicates that the upper 30 cm of unit 7 did not represent the top of a soil horizon developed above underlying loess deposits, but that this part of unit 7 likely resulted from a progressive rise in the aeolian sedimentation, whereas pedological processes were still very weak.

6.1.3. Cycle 3 (thickness: ca. 1.4 m)

Cycle 3 extends from the upper part of unit 7 to the middle of unit 4 (Surduk soil). It is characterised by an inverted asymmetrical pattern starting with a progressive increase in GSI, fine and coarse sand percentages, to a maximum just below the lower boundary of unit 4, and ending with a rapid decrease within the Surduk soil. The upper boundary of Cycle 3 is underlined by a slight increase in clay percentage, and a strong increase in TOC percentages (from 0.25 to 0.50).

6.1.4. Cycles 4–8

These five grain size cycles are presented together as they do not show any link with marked stratigraphical boundaries. They occur within the apparently homogeneous loess of units 3 and 2 between the top of the Surduk soil and the base of the topsoil. Cycle 4 corresponds to unit 2 and Cycles 5–8 to unit 2.

These cycles are separated from the underlying ones by a very marked shift of all the grain size parameters at the top of the Surduk soil due to the stronger aeolian dynamics during the Upper Pleniglacial. Cycles 4–5 are asymmetric and show more than 5% increasing peaks in the GSI and fine sand percentages at their basis. Cycles 6, 7 and 8 are then materialised by a strong increase in the fine sand percentages, whereas the GSI shows only smoothed peaks.

The trend of the grain size median is to an increase during Cycle 4 to the base of Cycle 5, then to a decrease from the base of Cycles 5–7, and finally to an increase during Cycle 8. The trend of the clay percentage is opposite to this of the grain size median, except during Cycle 8. It shows a decrease from 15% to 10% from Cycle 4 to the basis of Cycle 5, and then an increase to 20% at the end of Cycle 8. The evolution of clay percentage also appears smoother than that of coarse grain percentage. These trends likely indicate a global decrease in the wind intensity from the basis (Cycle 5) to the top (Cycle 8) of unit 2.

The record of coarse particles ($>63\,\mu m\,\%$) shows that high amounts of coarse sands ($>160\,\mu m$) appear mainly within the Lower Pleniglacial loess and in the sandy loess below soil unit 7. Variations in coarse and fine sand percentages show no particular correlation along the stratigraphy. Indeed, during the Upper Pleniglacial strong peaks characterise the fine sand curve, whereas coarse sand percentages remain stable and very low. Taking into account that these fine sand peaks indicate periods of stronger winds in both Lower and Upper Pleniglacial loess units, the differences between coarse and fine sand records could indicate:

1 The prevalence of markedly higher wind speed during the Lower Pleniglacial, able to drift coarse sand grains from the part of the Danube braided fluvial system located to the east of the Fruška Gora Mountain at about 15–18 km NNW of the profile) or
2 The occurrence of very strong episodes of NE winds (NE storms) during the Lower Pleniglacial able to drift coarse sand grains from the Danube plain, ENE of Surduk.

6.2. Comparison with other loess grain size records

The most complete and best dated record suitable for comparison in Serbia is the Titel plateau sequence located 20 km to the north of Surduk (Marković et al., 2008; Bokhorst et al., 2006, this issue). The comparison between the stratigraphical and grain size records from Surduk and Titel ($>44\,\mu m\,\%$) shows similar trends in their grain size records (Fig. 8). This observation implies that the main variations in wind dynamics during the last climatic cycle have at least a regional significance. In parallel, the homogeneity of both pedosedimentary budgets (19 and 20 m, respectively) and stratigraphical records support that there was no significant difference in the response of the environments during the last climatic cycle between the two sites separated by ca. 20 km (Fig. 8).

Even if Last Interglacial and Early Glacial pedosedimentary budgets are very close in both sequences, a more detailed approach reveals strong differences in the relative thickness of loess deposits. For example, the Lower Pleniglacial (L1L2) is markedly thicker in Titel and represented by four subsequences instead of one in Surduk. Except at the end of the Upper Pleniglacial loess (Cycle 8), the same observation can be made for the Middle and Upper Pleniglacial periods, the latter being especially more developed at Surduk. These differences can be attributed to local geomorphological contexts as suggested by Bokhorst et al. (2006) and Bokhorst et al. (this issue). For example, the exceptional thickness of the Lower Pleniglacial loess in Titel is due to the presence of a paleodepression absent in Surduk.

This last observation underlines that loess–palaeosol sequences are composed of discontinuous phases of aeolian deposition triggered by high-frequency wind regime variations and that the record of each of these phases is also highly dependent on the local geomorphological conditions: existence of sedimentary traps as palaeodepressions or valleys, location of the site compared to local coarse sediments sources and dominant winds. Furthermore, the shape of the fine sand curve including Cycles 7 and 8 at Surduk can be compared with that in the other west-European Upper Pleniglacial grain size records, where a strong grain size decrease dated at about 22 ka is followed by a last increase in loess grain size peaking around 17–16 ka (Rousseau et al., 2002; Antoine et al., submitted).

Finally, even if it is clear that the main trends in stratigraphy and grain size are recorded over a huge area in Europe during the last climatic cycle, detailed correlations at the level of sub-cycles and of millennial events are still very difficult owing to local variations in loess sedimentation rate and to the actual degree of accuracy of available dating methods.

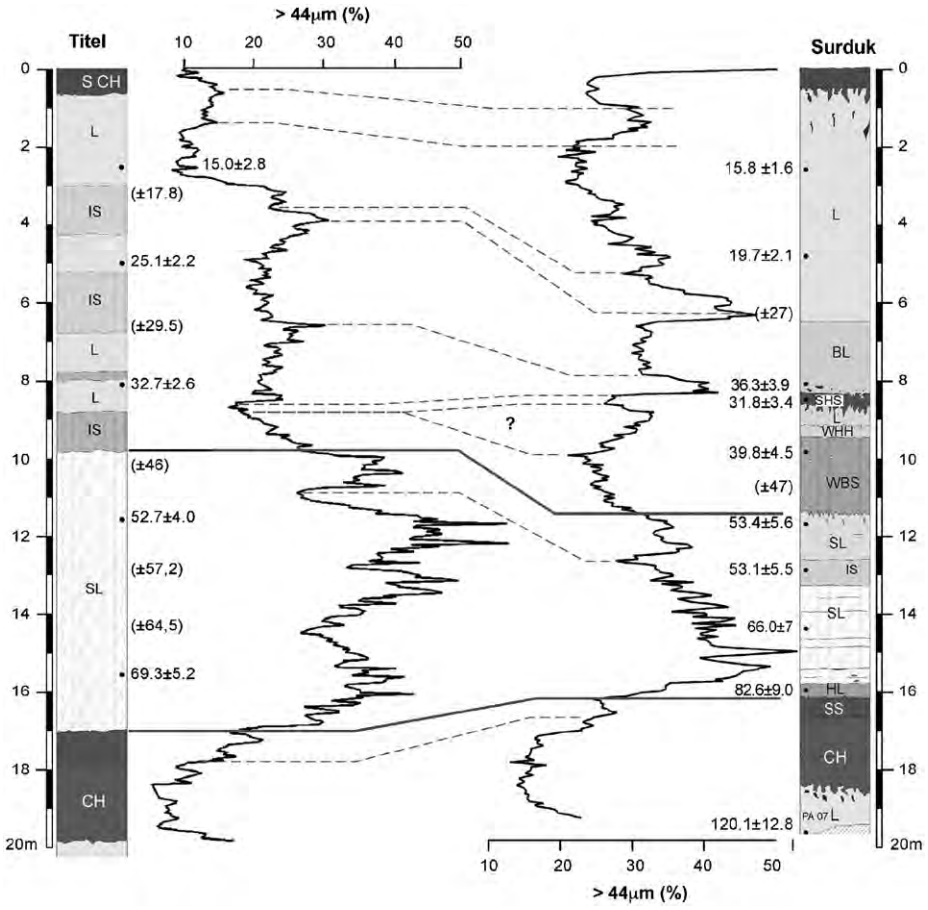

Fig. 8. Comparison between the >44 μm% curves from Surduk and Titel (Titel data according to Bokhorst et al., 2006; Marković et al., 2008) (see Fig. 7 for abbreviations).

6.3. Comparison with Greenland dust records

The analysis of the high-resolution grain size variations allow to evidence a succession of short periods of coarse loess sedimentation, named Loess Events (LE), within the Upper loess (units 2 and 3; L1–L1). They are defined according to the methodology developed for the interpretation of the grain size records from the Nussloch loess sequence (Rousseau et al., 2002, 2007; Antoine et al., 2003a, submitted).

According to dating results and sedimentation rates from studies of other European Upper Pleniglacial loess series, the Loess Events correspond to millennial-timescale climatic events (Rousseau et al., 2002, 2007; Antoine et al., 2003a). They show that wind intensity experienced strong and high-frequency variability during this period that corresponds to the main phase of loess accumulation in Europe (Frechen et al., 2003), and to the main period of dust concentration in the Greenland ice cores (GRIP Members, 2003; NGRIP, 2004; Ruth et al., 2006).

Based on the dating results, a comparison between the records of the loess grain size in Surduk and of the dust content in Greenland ice-core (GRIP) is proposed (Fig. 9). Strong variations in loess sedimentation rates and error bars on age estimates are still limiting the resolution of such comparisons. However, the main periods of loess deposition observed in Surduk are clearly contemporaneous with the main periods of dust concentration in Greenland around 60±5 and 25±5 ka as already demonstrated in Western Europe (Rousseau et al., 2002).

According to the study of the Nussloch loess sequence, the cold episodes in the North Atlantic area (DO stadials) are supposed to correspond, on the continent, to the loess deposition intervals, in cold, dry and windy conditions, while the warm phases (DO interstadials) are considered to correspond to milder and moister conditions, allowing the development of soil horizons. In the south of the Carpathian Basin, this correlation methodology can hardly be applied owing to the prevalence of very arid conditions during the whole Last Glacial period characterised in the loess record by the absence of well-expressed soil horizons and of tundra gley layers (Figs. 7 and 9).

7. Conclusions

The Surduk section yields one of the most complete and best preserved record of the last climatic cycle in Serbia. The stratigraphical approach coupled with high-resolution

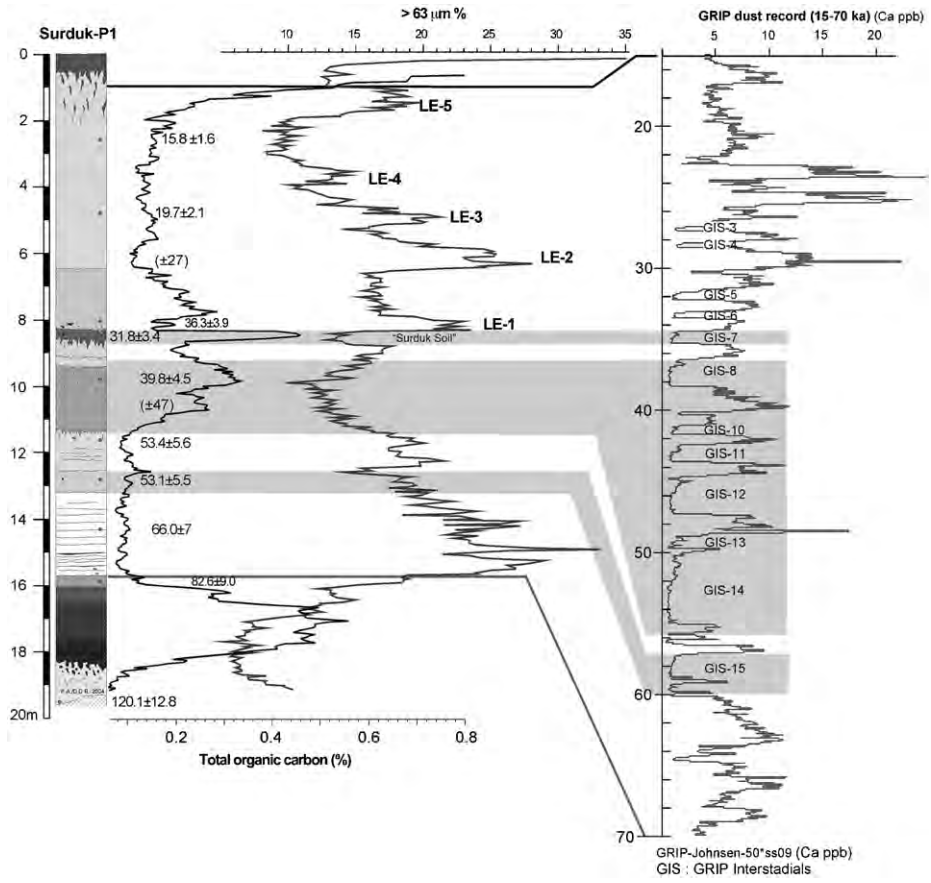

Fig. 9. Attempt in correlation between the variations of the main grain size parameters at Surduk (GSI and % > 63 µm), and the dust record from GRIP (GRIP chronology according to Johnsen et al., 2001).

grain size, magnetic susceptibility and total organic carbon analysis and IR-OSL dating allows proposal of a detailed and well-dated record of environmental and climatic changes during the last climatic cycle (Upper Pleistocene). The main conclusions are:

1. Comparison between Surduk and other local or European sequences shows that the response of loessic environments south of the Carpathian Basin is very homogeneous and that the preserved stratigraphical pattern is regionally the same in loess records from the European loess belt. Such a uniform response over thousands of kilometres, while the transported material originated from various sources, indicates that this stratigraphical pattern is driven by major climatic shifts during the last climatic cycle.

   The Surduk sequence shows nevertheless a markedly drier environment during the whole last climatic cycle, as shown by the lack of features characteristic of ice-rich permafrost (ice wedges, tundra gleys) and by the pedological character of soils (mainly humic).
2. IR-OSL dating results indicate that the main environmental change, between the basal humic soil complex and the onset of loess sedimentation, is likely to correspond to the MIS 5/4 boundary at ca. 75 ka (Martinson et al., 1987), as in west-, central and east-European loess sequences (Rousseau et al., 1998, 2001; Antoine et al., 1999, 2001). In addition, estimated sedimentation rates show a strong increase during the younger part of the Upper Pleniglacial, and support the results obtained from Central Europe (Frechen et al., 2003), implying that the general timing of loess deposition in Europe is rather homogenous.
3. Comparison between the clay, TOC, MS and coarse particle variations allows reinforcing the differentiation between the various soil and soil complexes within the sequence. If the Basal soil complex is characterised by the highest values in TOC, clay and MS, the middle Pleniglacial brown soils show only a relative enrichment in clay and TOC whereas MS remains very low. The combination of clay, TOC and MS variations is thus very useful to define an accurate sedimentological signature of the various types of soils (Chernozem, cambic horizons) and can be used as a good proxy for local temperature and moisture reconstructions.
4. The variations of the grain size index (GSI) and of the fine sand percentage along the sequence show that loess sedimentation was not homogeneous during the Last Glacial, and that it was characterised by a succession of short events marked by stronger aeolian dynamics and

higher sedimentation rates. These millennial-timescale events, already observed in west-European loess sequences, are related to abrupt increases in the aeolian dynamics, especially during the Upper Pleniglacial. This observation shows that the rapid climatic variability, which characterises the North Atlantic and Greenland areas, is also imprinted in the loess of the southern edge of the European loess belt. Finally, the variations in both coarse and fine sand percentages along the sequence show a contrasting pattern between the Lower and Upper Pleniglacial periods, raising questions about the prevailing wind regime during these periods, either strong dust storms able to drift coarse sand grains from the NNW, or significant periodical changes of the dominant winds to the NE.

Acknowledgements

This paper includes contributions LDEO-7212 and LSCE-3674. This study was funded by the CNRS ECLIPSE programme and by the French–Serbian Pavle Savic exchange programme. The authors thank N. Catto for the final revision of the English text and the anonymous reviewers for their constructive remarks.

References

Antoine, P., Rousseau, D.D., Lautridou, J.P., Hatté, C., 1999. Last Interglacial–Glacial climatic cycle in loess–paleosol successions of north-western France. Boreas 28, 551–563.

Antoine, P., Rousseau, D.D., Zöller, L., Lang, A., Munaut, A.V., Hatté, C., Fontugne, M., 2001. High-resolution record of the last interglacial–glacial cycle in the Nussloch loess palaeosol sequences, Upper Rhine Area, Germany. Quaternary International 76–77, 211–229.

Antoine, P., Rousseau, Hatté, C., Zöller, L., Lang, A., Fontugne, M., Moine, O., 2003a. Événements éoliens rapides en contexte loessique: l'exemple de la séquence du Pléniglaciaire supérieur weichselien de Nussloch (Vallée du Rhin-Allemagne). Quaternaire 13 (3–4), 199–208.

Antoine, P., Bahain, J.-J., Debenham, N., Frechen, M., Gauthier, A., Hatté, C., Limondin-Lozouet, N., Locht, J.-L., Raymond, P., Rousseau, D.-D., 2003b. Nouvelles données sur le Pléistocène du Nord du Bassin Parisien : les séquences loessiques de Villiers-Adam (Val d'Oise, France). Quaternaire 14, 219–235.

Antoine, P., Rousseau, D.D., Kunesch, S., Hatté, C., Lang, A., Zöller, L., Moine, O. (submitted). Evidence of rapid and cyclic eolian deposition during the Last Glacial in European loess series (Loess Events): the high-resolution records from Nussloch (Germany). Quaternary Science Reviews.

Bard, E., 1998. Geochemical and geophysical implications of the radiocarbon calibration. Geochimica et Cosmochimica Acta 62, 2025–2038.

Bard, E., Arnold, M., Hamelin, B., Tisnerat-Laborde, N., Cabioch, G., 1998. Radiocarbon calibration by means of mass spectrometric $^{230}Th/^{234}U$ and ^{14}C ages of corals. An updated data base including samples from Barbados, Mururoa and Tahiti. Radiocarbon 40 (3), 1085–1092.

Bibus, E., 1980. Zur Relief-, Boden- und Sedimententwicklung am unteren Mittelrhein. Frankfurter Geowissenschaftliche Arbeiten, Series D (296pp.)

Bokhorst, M.P., Vandenberghe, J., Marković, S.B., Gaudenyi, T., 2006. The Late Pleistocene loess–paleosol sequence at Titel Old Brickyard exposure. Danubius Pannonico Mysicus-Space of Challenges, Field trip Guide Book, Danuble Loess Meeting, Novi Sad, October 2006, pp. 32–34.

Bokhorst, M.P., Beets, C.J., Marković, S.B., Gerasimenko, N.P., Matviishina, Z.N., Frechen M., 2008. Pedo-chemical climate proxies in late Pleistocene Serbian–Ukranian loess sequences. Quaternary International, doi:10.1016/j.quaint.2008.09.003.

Bronger, A., 1976. Zur quartaeren Klima- und Landschaftsgeschichte des Karpatenbeckens auf palaeopedologischer und bodengeographischer Grundlage. Kieler Geographische Schriften 45, 1–268.

Bronger, A., Pant, R.K., Singhvi, A.K., 1985. Micromorphology, mineralogy, genesis and dating of loess-paleosol sequences and their application to Pleistocene chronostratigraphy and paleoclimate: a comparison between Southeast Central Europe and the Kashmir Valley/Central Asia. Aspect of Loess Research China (Ocean Press), 121–129.

Bronger, A., 2003. Correlation of loess–paleosol sequences in East and Central Asia with SE Central Europe: towards a continental Quaternary pedostratigraphy and paleoclimatic history. Quaternary International 106/107, 11–31.

Ding, Z.L., Ren, J.Z., Yang, L.S., Liu, T.S., 1998. Climatic instability during the Penultimate Glaciation: evidence from two high-resolution loess records, China. Journal of Geophysical Research 104, 123–132.

Ding, Z.L., Derbyshire, E., Yang, S.L., Yu, Z.W., Xiong, S.F., Liu, T.S., 2002. Stacked 2.6-Ma grain size record from the Chinese loess based on five sections and correlation with the deep-sea $\delta^{18}O$ record. Paleoceanography 17, 5.1–5.21.

Dolecki, L., 1986. Differentiation of grain size of the Vistulian loesses on the Grzeda Horodelska Plateau (SE Poland). In: Maruszczak, H. (Ed.), Problems of the Stratigraphy and Paleogeography of Loesses. Maria Curie-Sklodowska University, Canada, pp. 165–178.

FAO, 2006. World reference base for soil resources: FAO World Soil Ressource Reports 103, Rome (145pp.).

Frechen, M., 1999. Upper Pleistocene loess stratigraphy in Southern Germany. Quaternary Geochronology 18, 243–269.

Frechen, M., Oches, E.A., Kohfeld, K.E., 2003. Loess in Europe—mass accumulation rates during the Last Glacial Period. Quaternary Science Reviews 22, 1835–1857.

Fuchs, M., Rousseau, D.D., Antoine, P., Hatté, C., Gauthier, C., 2007. Chronology of the Last Climatic Cycle (Upper Pleistocene) of the Surduk loess sequence, Vojvodina, Serbia. Boreas 37 (1), 66–73.

Gauthier, C., Hatté, C., 2007. Suitability and reliability of isotopic biogeochemistry studies in paleoclimatology: focus on protocols. European Geosciences Union General Assembly, EGU2007-A-02912, Vienne, Austria. Poster.

Gerasimenko, N., 2006. Upper Pleistocene loess–palaeosols and vegetational successions in the Middle Dnieper area, Ukraine. Quaternary International 149, 55–66.

GRIP Members, 1993. Climate instability during the last interglacial period recorded in the GRIP ice-core. Nature 364, 203–207.

Haesaerts, P., 1985. Les loess du Pléistocène Supérieur en Belgique; comparaison avec les séquences de l'Europe Centrale. Bulletin de l'Association Française pour l'Etude du Quaternaire 22, 105–115.

Haesaerts, P., Borziak, I., Chirica, V., Damblon, F., Koulakovska, L., van der Plicht, J., 2003. The east Carpathian loess record: a reference for the Middle and Late Pleniglacial stratigraphy in central Europe. Quaternaire 14, 163–188.

Hatté, C., Fontugne, M., Rousseau, D.D., Antoine, P., Zöller, L., Tisnerat-Laborde, N., Bentaleb, I., 1998. $\delta^{13}C$ variations of loess organic matter as a record of the vegetation response to climatic changes during the Weichselian. Geology 26, 583–586.

Hatté, C., Pessenda, L.C.R., Lang, A., Paterne, M., 2001. Development of an accurate and reliable ^{14}C chronology for loess sequences. Application to the loess sequence of Nußloch (Rhine valley, Germany). Radiocarbon 43 (2B), 611–618.

Heller, F., Evans, M.E., 1995. Loess magnetism. Reviews of Geophysics 33 (2), 211–240.

Johnsen, S.J., Dahl-Jensen, D., Gundestrup, N., Steffensen, J.P., Clausen, H.B., Miller, H., Masson-Delmotte, V., Sveinbjörnsdottir, A.E., White, J., 2001. Oxygen isotope and palaeotemperature records from six Greenland ice-core stations: Camp Century, Dye-3, GRIP, GISP2, Renland and NorthGRIP. Journal of Quaternary Science 16, 299–307.

Konert, M., Vandenberghe, J., 1997. Comparison of laser grain size analysis with pipette and sieve analysis: a solution for the underestimation of the clay fraction. Sedimentology 44, 523–535.

Kukla, G., 1977. Pleistocene land–sea correlations. 1. Europe. Earth-Science Reviews 13, 307–374.

Lang, A., Hatté, C., Rousseau, D.-D., Antoine, P., Fontugne, M., Zöller, L., Hambach, U., 2003. High-resolution chronologies for loess: comparing AMS ^{14}C and optical dating results. Quaternary Science Reviews 22, 953–959.

Lautridou, J.-P., 1985. Le cycle périglaciaire pléistocène en Europe du Nord-Ouest et plus particulièrement en Normandie. Thèse es Sciences, Univ. Caen, Centre de Géomorphologie Caen (908pp.).

Liu, T.S., 1985. Loess and the Environment. Ocean Press, Beijing, (251pp.).

Maher, B.A., Taylor, R.M., 1988. Formation of ultrafine-grained magnetite in soils. Nature 336, 368–370.

Maher, B.A., Alekseeva, A., Alekseevab, T., 2003. Magnetic mineralogy of soils across the Russian Steppe: climatic dependence of pedogenic magnetite formation. Palaeogeography, Palaeoclimatology, Palaeoecology 201, 321–341.

Marković, S.B., Heller, F., Kukla, G.J., Gaudenyi, T., Jovanović, M., Miljković, L.J., 2003. Magnetostratigraphy of Stari Slankamen loess section. Zbornik Radova Instituta Zageografiju 32, 20–28 (in Serbian with English summary).

Marković, S., Kostić, N., Oches, E.A., 2004. Paleosols in the Ruma loess section (Vojvodina, Serbia). Revista Mexicana de Ciencias Geologicas 21, 79–87.

Marković, S.B., McCoy, W.D., Oches, E.A., Savić, S., Gaudenyi, T., Jovanović, M., Stevens, T., Walther, R., Ivanisević, P., Galić, Z., 2005. Paleoclimate record in the Upper Pleistocene loess–paleosol sequence at Petrovaradin brickyard (Vojvodina, Serbia). Geologica Carpathica 56, 545–552.

Marković, S.B., Oches, E.A., Sümegi, P., Jovanović, M., Gaudenyi, T., 2006. An introduction to the Middle and Upper Pleistocene loess–paleosol sequence at Ruma brickyard, Vojvodina, Serbia. Quaternary International 149, 80–86.

Marković, S.B., Oches, E.A., McCoy, W.D., Gaudenyi, T., Frechen, M., 2007. Malacological and sedimentological evidence for "warm" climate from the Irig loess sequence (Vojvodina, Serbia). Geophysics, Geochemistry and Geosystems 8, Q09008.

Marković, S.B., Bokhorst, M., Vandenberghe, J., McCoy, W.D., Oches, E.A., Hambach, U., Gaudenyi, T., Jovanović, M., Zöller, L., Stevens, T., Machalett, B., 2008. Late Pleistocene loess–paleosol sequences in the Vojvodina region, North Serbia. Journal of Quaternary Science 23 (1), 73–84.

Martinson, D., Pisias, M.G., Hays, J.D., Imbrie, J., Moore, T.C., Shackleton, N.J., 1987. Age dating and the orbital theory of ice ages: development of a high-resolution 0 to 300,000-year chronostratigraphy. Quaternary Research 27, 1–29.

Moine, O., Rousseau, D.-D., Antoine, P., 2005. Terrestrial molluscan records of Weichselian Lower to Middle Pleniglacial climatic changes from the Nussloch loess series (Rhine Valley, Germany): the impact of local factors. Boreas 34, 363–380.

Moine, O., Rousseau, D.-D., Antoine, P., 2008. The impact of Dansgaard–Oeschger cycles on the loessic environment and malacofauna of Nussloch (Germany) during the Upper Weichselian. Quaternary Research 70, 91–104.

NGRIP Members, 2004. High resolution Climate Record of the Northern Hemisphere reaching into the Last Glacial Interglacial Period. Nature 431, 147–151.

Nugteren, G., Vandenberghe, J., van Huissteden, K., An, Z., 2004. A Quaternary climate record based on grain size analysis from the Luochuan loess section on the Central Loess Plateau, China. Global and Planetary Change 41, 167–183.

Rousseau, D.D., 1987. Paleoclimatology of the Achenheim series (middle and upper Pleistocene, Alsace, France). A malacological analysis. Palaeogeography, Palaeoclimatology, Palaeoecology 59, 293–314.

Rousseau, D.D., Soutarmin, N., Gaume, L., Antoine, P., Lang, M., Lautridou, J.P., Sommé, J., Zöller, L., Lemeur, I., Meynardier, L., Fontugne, M., Wintle, A., 1994. Histoire du Dernier cycle climatique enregistrée dans la séquence loessique d'Achenheim (Alsace, France), à partir de la susceptibilité magnétique. Comptes Rendus de l'Académie des Sciences, Paris 319 (Série II), 551–558.

Rousseau, D.D., Zöller, L., Valet, J.P., 1998. Climatic variations in the Upper Pleistocene loess sequence at Achenheim (Alsace, France). Based on a magnetic susceptibility TL chronology of loess. Quaternary Research 49, 255–263.

Rousseau, D.D., Gerasimenko, N., Matvviishina, Z., Kukla, G.J., 2001. Late Pleistocene environments of the Central Ukraine. Quaternary Research 56, 349–356.

Rousseau, D.-D., Antoine, P., Hatté, C., Lang, A., Zöller, L., Fontugne, M., Ben Othman, D., Luck, J.-M., Moine, O., Labonne, M., Bentaleb, I., Jolly, D., 2002. Abrupt millenial climatic changes from Nussloch (Germany) Upper Weichselian eolian records during the Last Glaciation. Quaternary Science Reviews 21, 1577–1582.

Rousseau, D.-D., Sima, A., Antoine, P., Hatté, C., Lang, A., Zöller, L., 2007. Link between European and North-Atlantic abrupt climate changes over the Last Glaciation. Geophysical Research Letters 34.

Ruth, U., Wagenbach, D., Steffensen, J.-P., Bigler, M., 2006. Continuous record of microparticle concentration and size distribution in the central Greenland NGRIP ice core during the Last Glacial period. Journal of Geophysical Research 108, 4098.

Schirmer, W., 2000. Rhine loess Ice Cores and deep-sea cores during MIS 2-5. Zeitschrift der Deutschen Geologischen Gesellschaft 151, 309–332.

Semmel, A., 1997. Referenzprofile des Würmlösses im Rhein-Main-Gebiet. Jahresberichte der Wetterauischen Gesellschaft für die Gesamte Naturkunde zu Hanau 148, 37–47.

Shi, C., Zhu, R., Glass, B.P., Liu, Q., Zema, A., Suchy, V., 2003. Climate variations since the last interglacial recorded in Czech loess. Geophysical Research Letters 30 (11), 1562.

Singhvi, A.K., Bronger, A., Sauer, W., Pant, R.K., 1989. Thermoluminescence dating of loess–paleosol sequences in the Carpathian Basin: a suggestion for a revised chronology. Chemical Geology (Isotope Geoscience Section) 73, 307.

Sommé, J., Paepe, R., Lautridou, J.P., 1980. Principes, méthodes et système de la stratigraphie du Quaternaire dans le Nord-Ouest de la France et la Belgique. In: Problèmes de stratigraphie quaternaire en France et dans les pays limitrophes, Supplément au Bulletin de l'Association Française pour l'Etude du Quaternaire NS-1, pp. 148–162.

Sun, J., Huang, X., 2006. Half-precessional cycles recorded in Chinese loess: response to low-latitude insolation forcing during the Last Interglaciation. Quaternary Science Reviews 25, 1065–1072.

Vandenberghe, J., An, Z., Nugteren, G., Huayu, L., Van Huissteden, K., 1997. New absolute timescale for the Quaternary climate in the Chinese loess region by grain-size analysis. Geology 25 (1), 35–38.

Vandenberghe, J., Huijzer, B., Mücher, H., Laan, W., 1998. Short climatic oscillations in a western European loess sequence (Kesselt, Belgium). Journal of Quaternary Science 13, 471–485.

Van Vliet-Lanoë, B., 1987. Le rôle de la glace de ségrégation dans les formations superficielles de l'Europe du Nord-Ouest. Thèse de Doctorat d'Etat, Université Paris I (864pp.)

Veklitch, M.F., 1979. Pleistocene loesses and fossil soils of the Ukraine. Acta Geologica Scientiarum Hungaricae 22, 35–62.

Xiao, J., Porter, S.C., An, Z., Kumai, H., Yoshikawa, S., 1995. Grain size of quartz as an indicator of winter monsoon strength on the Loess Plateau of Central China during the last 130 000 yr. Quaternary Research 43, 22–29.

Zöller, L., Stremme, H.E., Wagner, G.A., 1988. Thermolumineszenz-Datierung an Löß-Paläoboden-Sequenzen von Nieder-, Mittel- und Oberrhein. Chemical Geology (Isotope Geoscience Section) 73, 39–62.

Zöller, L., Oches, E.A., McCoy, W.D., 1994. Towards a revised chronostratigraphy of loess in Austria with respect to key sections in the Czech Republic and in Hungary. Quaternary Geochronology (Quaternary Science Reviews) 13, 465–472.

Zöller, L., Rousseau, D.D., Jäger, K.D., Kukla, G., 2004. Last interglacial, Lower and Middle Weichselian—a comparative study from the Upper Rhine and Thuringian loess areas. Zeitschrift für Geomorphologie N.F. 48, 1–24.